Clinical Science (2021) **135** 2127–2142
https://doi.org/10.1042/CS20210644

PORTLAND PRESS

Research Article

Key role for EphB2 receptor in kidney fibrosis

Zhimin Huang[1,2], Simeng Liu[1], Anna Tang[1], Laith Al-Rabadi[1], Mark Henkemeyer[3], Patrice N. Mimche[4] and Yufeng Huang[1]

[1]Department of Internal Medicine, Division of Nephrology and Hypertension, University of Utah Health Science, Salt Lake City, UT, U.S.A.; [2]Department of Internal Medicine, Division of Nephrology, Nanjing Medical University, Jiangsu Province Hospital, Nanjing, China; [3]Department of Neuroscience, University of Texas Southwestern Medical Center, Dallas, TX, U.S.A.; [4]Department of Pathology, Division of Microbiology and Immunology, Molecular Medicine Program, University of Utah Health Science, Salt Lake City, UT, U.S.A.

Correspondence: Yufeng Huang (Yufeng.huang@hsc.utah.edu) or Patrice N. Mimche (Patrice.mimche@path.utah.edu) or Mark Henkemeyer (mark.henkemeyer@utsouthwestern.edu)

Erythropoietin producing hepatocellular (Eph)–Eph receptor interacting (Ephrin) receptor–ligand signaling has been implicated in the development of tissue fibrosis, though it has not been well defined in the kidney. We detected substantial up-regulation of expression and phosphorylation of the EphB2 receptor tyrosine kinase in fibrotic kidney tissue obtained both from mice subjected to the unilateral renal ischemia–reperfusion (IR) model at 14 days and in patients suffering from chronic kidney disease (CKD). Knockout (KO) mice lacking EphB2 expression exhibited a normal renal structure and function, indicating no major role for this receptor in kidney development or action. Although IR injury is well-known to cause tissue damage, fibrosis, and renal dysfunction, we found that kidneys from *EphB2*KO mice showed much less renal tubular injury and retained a more preserved renal function. IR-injured kidneys from *EphB2* KOs exhibited greatly reduced fibrosis and inflammation compared with injured wildtype (WT) littermates, and this correlated with a significant reduction in renal expression of profibrotic molecules, inflammatory cytokines, NADPH oxidases, and markers for cell proliferation, tubular epithelial-to-mesenchymal transition (EMT), myofibroblast activation, and apoptosis. A panel of 760 fibrosis-associated genes were further assessed, revealing that 506 genes in WT mouse kidney following IR injury changed their expression. However, 70.9% of those genes were back to or close to normal in expression when *EphB2* was deleted. These data indicate that endogenous EphB2 expression and signaling are abnormally activated after kidney injury and subsequently contribute to the development of renal fibrosis via regulation of multiple profibrotic pathways.

Introduction

Chronic kidney disease (CKD) is characterized by persistent inflammation and a gradual increase in fibrosis including glomerulosclerosis and tubulointerstitial fibrosis, ultimately leading to end-stage renal disease (ESRD) regardless of the underlying disorder [1]. This points to a final common pathway for ESRD. A better understanding of the key mediators of this common pathway will potentially result in the design of more targeted therapies to prevent or reverse the progression of CKD.

Erythropoietin producing hepatocellular (Eph) receptor tyrosine kinases and their corresponding Eph receptor interacting (Ephrin) ligands form a large family of highly conserved membrane-anchored signaling proteins that control diverse cell–cell interactions throughout development and in adult life [2]. Upon cell–cell contact, EphB–EphrinB interactions in particular result in dimers, tetramers, and higher order protein clusters, leading to the activation of bidirectional signaling cascades that are propagated into the receptor-expressing cell (forward signaling) and the ligand-expressing cell (reverse signaling) [3–5]. Given that Eph–Ephrin bidirectional signaling is thought to participate in a broad array of cell–cell interactions, migration, and adhesion events during both embryonic development and during physiological tissue repair [2,6–10], it is not surprising that dysregulation of these molecules has been implicated

Received: 21 June 2021
Revised: 24 August 2021
Accepted: 27 August 2021

Accepted Manuscript Online: 31 August 2021
Version of Record published: 10 September 2021

Clinical Science (2021) **135** 2127–2142
https://doi.org/10.1042/CS20210644

in tissue fibrosis. Indeed, roles for EphB–EphrinB signaling in tissue fibrogenesis have been uncovered in multiple mouse models of vascular [11], cardiac [12], skin [13], lung [14], and liver fibrosis [15,16]. However, the potential functions for these receptors and ligands with respect to pathophysiology of the kidney are largely unknown.

In the adult renal glomeruli, EphrinB1 is localized at the slit diaphragm of the podocyte in glomeruli [17], EphrinB2 is mainly expressed in glomerular endothelial cells (ECs) and arterial smooth muscle [18], whereas EphrinB3 is barely detectable [19]. Glomerular expression or distribution of Eph receptors is still unclear although a few studies indicated that a rare cell expresses EphB4 in mature glomeruli [18]. In renal tubules, EphrinB1 is detected throughout the whole nephron and might affect the cytoarchitecture of tubular epithelial cells [19]. Besides being expressed in arterial smooth muscle cells and ECs, EphrinB2 was also found abundantly in connecting tubules and cortical and medullary collecting ducts of developing and adult kidneys [18]. EphB2 receptor was found to be expressed abundantly in the tubules of the inner and outer medulla, including the distal straight tubules and the thin limb of the loop of Henle where it is concentrated in the basal side of cells. EphB4 expression is restricted to the capillaries in the medulla. EphB6 is preferentially expressed in the renal corpuscles and tubules of both the cortex and the outer medulla, including the proximal and distal tubules. However, EphB6 itself lacks catalytic activity and it is unlikely to operate as an independent receptor but rather signals as part of a hetero-oligomeric signaling complex with other EphB receptors *in vivo* [20].

It was previously reported that EphrinB2 reverse signaling protected against capillary rarefaction and fibrosis after kidney injury induced by unilateral ureteral obstruction (UUO) or ischemia–reperfusion (IR) injury, since mice lacking EphrinB2-PDZ-dependent signaling had more severe vascular injury and enhanced fibrosis after kidney injury [21]. However, it is also possible that the PDZ-dead EphrinB2 protein acts as stronger ligand to stimulate EphB forward signaling, and this might be the cause of the excessive kidney fibrosis observed in the above study. Further, the above study did not determine which, if any, EphB receptor participates in kidney pathology after injury. Given the important profibrotic role of EphB2 signaling observed recently in liver fibrosis [15,16] and the most abundant expression of EphB2 in kidney tubular cells [19], we hypothesize that EphB2 is likely involved in renal fibrosis. In the present study, we investigated whether elevated EphB2 is also observed in different kidney diseases and whether expression and signaling of EphB2 are involved in the development of renal fibrosis using EphB2 knockout (KO) and littermate control mice to receive unilateral renal IR injury. We showed that EphB2 expression and signaling capacity are significantly up-regulated following IR injury in a mouse model and in kidneys from experimental hypertensive and diabetic CKD mouse models and patients suffering from CKD. Moreover, genetic loss of *EphB2* in KO mice strongly protected kidneys from IR injury-induced renal damage, dysfunction, and fibrosis, thus identifying a crucial role for this receptor in mediating the adverse cellular events that impact the kidney during disease progression.

Materials and methods

Reagents

Unless specified otherwise, all other reagents were purchased from Sigma Chemical Co. (St. Louis, Missouri, U.S.A.).

Animals

Gene targeted KO mice lacking expression of EphB2 [3] (generated by Dr. Henkemeyer in University of Texas Southwestern Medical Center, Dallas, TX) were maintained on a C57BL/6J background and were bred in-house under a $EphB2^{+/-}$ heterozygous breeding system to generate $EphB2^{-/-}$ homozygous mutants and $EphB2^{+/+}$ wildtype (WT) control littermates (mouse breeding and genotyping were performed at Dr. Mimche's laboratory in University of Utah). Animal maintenance and study procedures described below were performed at Dr. Huang's laboratory in University of Utah. All mice were given water and food *ad libitum*. Animal housing and care were in accordance with the NIH Guide for the Care and Use of Laboratory animals. The breeding, maintenance, and study of animals described herein were approved and carried out according to protocols approved by the Institutional Animal Care and Use Committee of University of Utah.

Experimental design

Homozygous male $EphB2^{-/-}$ mutant mice (n=5) and $EphB2^{+/+}$ WT male littermate control mice (n=5) aged 12 weeks were included in the study and received unilateral renal IR surgery. Briefly, mice were anesthetized with 2.5% isoflurane and unilateral renal ischemia was induced by application of microvascular clamps on right renal pedicles for 35 min, without contralateral nephrectomy. After the corresponding ischemia time, the clamp was released to initiate reperfusion and the incisions were closed surgically. This kidney was named as the IR-injured kidney (IR). The contralateral kidney (CTL) which did not undergo surgery served as normal uninjured control. All mice received

normal diet and normal drinking water and were killed under isoflurane anesthesia at 2 weeks after IR surgery. Blood samples were obtained by cardiac puncture for the measurement of BUN and creatinine (Cr) levels. Two kidneys of each mouse were perfused through the heart with 30 ml of cold phosphate-buffered saline (PBS) and weighted individually. Then, superior and inferior poles in each kidney were either snap-frozen in 2-methylbutane at −80°C or fixed in 10% neutralized formalin for histological examination. The remaining tissue was equally divided into two pieces and quickly frozen in liquid nitrogen and stored at −70°C until analysis of mRNA and protein expression by real-time RT-PCR and Western blotting.

Determination of renal function

Serum BUN and Cr concentrations were measured by using the QuantiChrom™ urea assay kit and creatinine assay kit (BioAssay System, Hayward, CA, U.S.A.).

Histological analyses

All microscopic examinations were performed in a blinded fashion. Three-micrometer sections of paraffin-embedded kidney tissues were stained with Periodic Acid–Schiff (PAS) and Masson's Trichrome. The tubular features such as brush border loss, dilatation, intraluminal cast, disappeared physical back to back position with enlarged spaces in between, interstitial inflammatory cell infiltration, and epithelial cell apoptosis were quantified as tubular injury by a computer-assisted method as previously described [22,23]. Masson's Trichrome-stained tissue sections were viewed with bright field illumination at 200× magnification. Ten non-overlapping fields of renal tubulointerstitial area were scored with a semi-quantitative ordinal scale (grade 0 for collagen/parenchyma % ≤5%; grade 1 for >5 to ≤25%; grade 2 for >25 to ≤50%; and grade 3 for >50%) and the mean used as the fibrosis score.

Immunofluorescent (IF) staining was performed and quantified on frozen renal sections as described previously [22,24]. Briefly, after blocking, frozen kidney sections incubated overnight at 4°C with the following primary antibodies: goat anti-human/mouse EphB2 antibody, clone AF467 (cat. # AF467, R&D Systems, Minneapolis, MN, U.S.A.), rabbit anti-phospho-EphB1/EphB2$^{Y594+Y596}$ ab61791 (Abcam, Cambridge, U.K.), rat anti-mouse F4/80 IgG (Cl:A3-1, Bio-Rad Laboratories, Inc., Hercules, CA, U.S.A.), and monoclonal rat anti-Ki-67 antibody, clone SolA15 (cat. # 14-5698-82, Invitrogen, Carlsbad, U.S.A.). Kidney sections were then stained with NorthernLights™ NL557-conjuated donkey anti-goat IgG (cat. # NL001, R&D), Alexa Fluor 594-conjugated donkey anti-rabbit IgG (cat. # A-21207, Invitrogen), and CyTM3-conjugated goat anti-rat IgG (cat. # 112-165-143, Jackson ImmunoResearch Laboratories Inc., West Grove, A, U.S.A.) as secondary antibodies for 1 h. Control slides treated with antibody diluent instead of primary antibody showed no staining. For immunostaining of α-smooth muscle action (α-SMA), FITC-conjugated mouse anti-α-SMA antibody (cat.# F3777) was used directly. After staining, one drop of 4′,6-diamidino-2-phenylindole (DAPI)-Fluoromount-G (cat. # 0100-20, SouthernBiotech, Birmingham, AL, U.S.A.) was applied on the section to counterstain the nucleic DNA. Ten random fields from each section were analyzed under ×200 magnification. Digital morphometric measurement of F4/80 or Ki-67-positive cells or α-SMA positive staining was quantified separately using ImageJ (National Institutes of Health, Bethesda, Maryland, U.S.A.).

Western blot analysis

Equal amounts of kidney tissue (15 mg) from each kidney of each group were homogenized in lysis buffer (Cell Signaling Technology, Inc., Beverly, MA, U.S.A.) with 1% NP40, 1 mM PMSF, and 1 tablet/5 ml protease inhibitor mix (Complete, Mini; Roche Diagnostics Corporation, Indianapolis, IN, U.S.A.). Protein sample from each kidney of each group at equal amount was pooled to represent the individual group for further examination. For Western blot analysis, protein samples (30 μg each) were subjected to SDS/PAGE in 4–12% gradient gel (Invitrogen) and immunoblotted on Immobilon-P transfer membranes (Millipore Corporation, Bedford, MA, U.S.A.). Proteins of EphB2, phospho-EphB1/EphB2$^{Y594+Y596}$, fibronectin (FN), α-SMA, N-cadherin, nuclear factor κ-B-p65 unite (NF-κB-p65), NADPH oxidase gp91^{phox} (Nox2) and its cofactor, p47^{phox}, phospho-Akt, and phosphorylated and total extracellular signal-regulated kinase 1/2 (ERK1/2) were assessed on the Western blots and the immunostaining band was visualized and quantitated as described [16,22,23]. All blots were run at least three times.

RNA preparation and real-time RT-PCR assay

Total RNA was extracted from kidney tissue using TRIzol reagent (Invitrogen) according to the manufacturer's instructions. Two micrograms of total RNA were reverse-transcribed using the Superscript III First-Strand synthesis

Clinical Science (2021) **135** 2127–2142
https://doi.org/10.1042/CS20210644

system for RT-PCR kit (Invitrogen). Real-time RT-PCR was performed using the SYBR Green Dye I (Applied Biosystems, Foster City, CA, U.S.A.) and the ABI 7900 Sequence Detection System (Applied Biosystems) as described previously [22]. Samples were run as triplicates in separate tubes to permit quantification of the target gene normalized to GAPDH. Sequences of primers used for rat and human *EphB* and Ephrin-B (*efnB*) molecules were listed in the Supplementary Table S1. Sequences of primers used for other molecules were described previously [16,22]. The specificity of the PCR products was confirmed using a 1.5% agarose gel by showing a specific single band with the expected size.

Apoptosis analysis

Kidney apoptosis was determined using a fluorescein isothiocyanate-labeled *in situ* TdT-mediated dUTP Nick-End Labeling (TUNEL) assay (cat. # 11684795910, Roche Molecular Biochemicals, Mannheim, Germany). Tissue sections of 3 μm were counterstained with DAPI and then examined by a fluorescence microscope. The apoptotic cells were counted and expressed as the number of TUNEL-positive cells per 100 cells in 10 randomly selected higher power fields.

NanoString gene expression assay

To further uncover the molecules that are regulated by EphB2 signaling and related to profibrotic pathway, the gene set expression was then quantified in RNA isolates described above using NanoString platform with the mouse nCounter Fibrosis Panel (NanoString Technologies, Inc., Seattle, WA, U.S.A.). This panel includes 10 internal reference genes and 760 targeted genes across 51 annotated pathways such as autophagy, oxidative stress, mitogen-activated protein kinase (MAPK) cell stress, NF-κB, complement activation, cytokine signaling, transforming growth factor-β (TGF-β), PDGF signaling, PI3K-Akt, epithelial-to-mesenchymal transition (EMT), apoptosis, angiogenesis, extracellular matrix (ECM) synthesis and degradation. These pathways are involved in the initial tissue damage response, chronic inflammation, proliferation of profibrotic cells, and tissue modification that leads to fibrosis. NanoString gene expression assay is a new platform for targeted gene expression including low-throughout gene based on molecular barcoding to quantify mRNA that does not require amplification [25]. Briefly, 100 ng of each total kidney RNA sample from the control lateral kidneys of WT mice (n=5) or IR-injured kidneys of WT mice (n=5) or EphB2$^{-/-}$ mice (n=5) were added to the codeset in a hybridization buffer and incubated at 65°C for 16 h. The codeset consisted of reporter and capture probes that hybridized the target sequences of interest, forming a tripartite complex on the NanoString nCounter™. After the assay, the raw counts for each gene were generated with nSlover™ (NanoString Technologies Inc.). Normalization of the data was performed using nSlover™ for the following two methods, (i) positive control normalization: gene expression data were normalized to the mean of the positive control probes for each assay (data from IR-injured WT mice served as positive controls); (ii) RNA content normalization: gene expression data were normalized to the geometric mean of reference genes in the codeset. This assay was carried out by the genomic core facility and analyzed by the bioinformatics core facility using the *limma* software at University of Utah and nSlover™ provided by the company.

Statistical analysis

All data are expressed as mean ± SD. Software Power for sample size calculation (www.clincalc.com) was used, based on the result of renal tubular injury score in a pilot study, which was 2.43 ± 0.15, as the primary readout. Power calculations assume the use of a two-sided, two-independent groups t test, with equal variance, and assuming the difference between means to be proportion of the standard deviation of the outcome measurement. Each group contains five mice. The study has at least 95% power to detect differences larger than 2.2 units of standard deviation between groups. Statistical analyses of differences among the groups were performed by two ways: ANOVA and subsequent Student–Newman–Keuls or Dunnett's testing for multiple comparisons. Comparisons with P-values <0.05 were considered significantly different.

Results

EphB2 is up-regulated and activated in the kidney after injury

Transcripts for all EphB and Ephrin-B molecules in the normal adult mouse kidney were assessed by RT-PCR (Supplementary Figure S1A), revealing the most prominent amplification products were *EphB2, EphB4, EphrinB1*, and *EphrinB2*. It has been shown that EphB4 is mainly expressed on vascular ECs and required for the structural integrity of blood vessels, and is not detected in the major kidney cells involved in fibrosis [21,26]. Furthermore, our data revealed that kidney tubular epithelial cells and tubular fibroblasts express the *EphB2* receptor and cognate *EphrinB1*

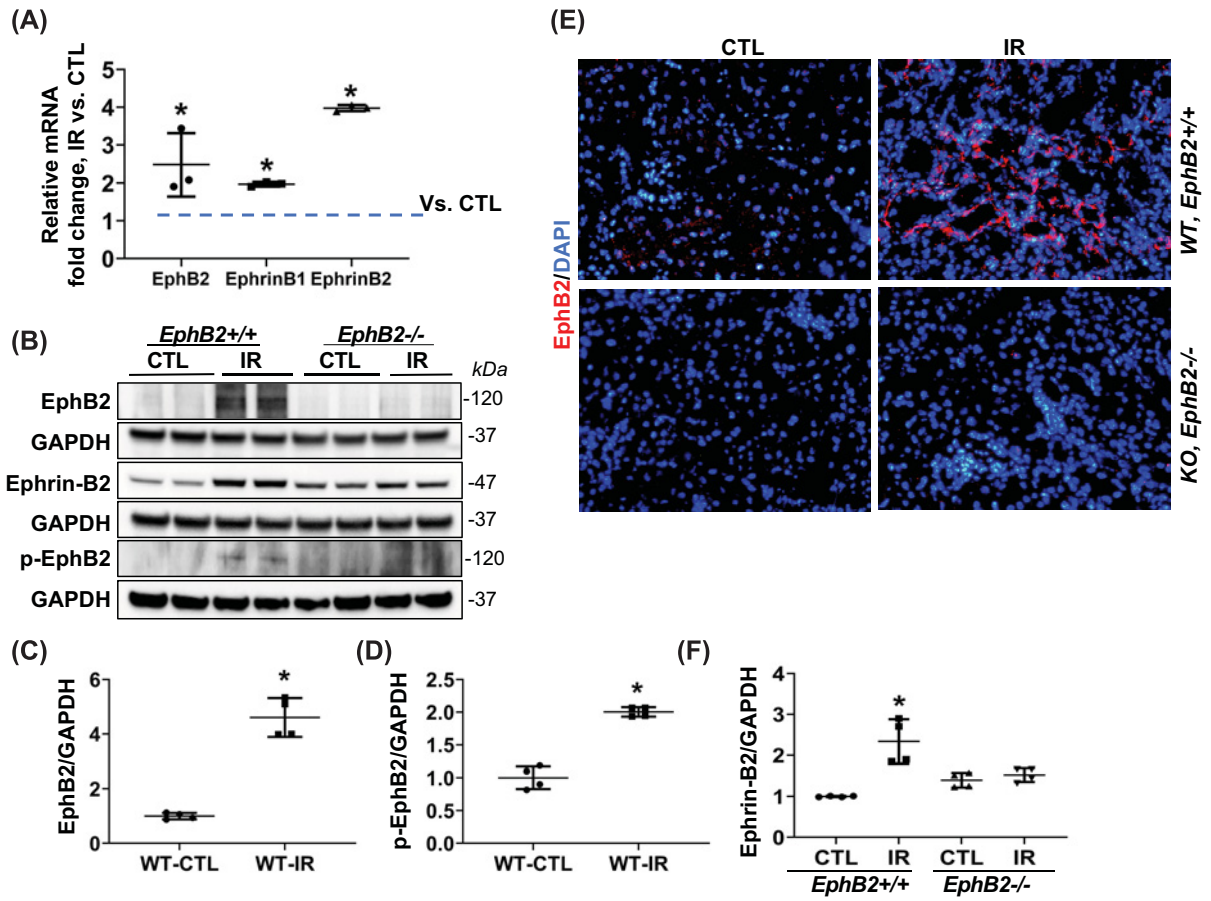

Figure 1. EphB2 expression increases in the kidney of mice following IR injury for 2 weeks

(**A**) EphB2 receptor, EphrinB1, EphrinB2 mRNA levels were analyzed in kidneys of mice using real time RT-PCR. Results are shown as fold change compared with contralateral kidneys (CTL). Error bars represent mean ± SD, n=5 animals. (**B**) Western blots of EphB2, phosphor-EphB2 (pEphB2^{Y594}), EphrinB2, and GAPDH from kidneys of *EphB2*$^{+/+}$ (WT) and *EphB2*$^{-/-}$ (KO) mice. Molecular weight was labeled on the right. The graphs summarize the results of band density measurements for EphB2 (**C**), p-EphB2 (**D**), and EphrinB2 (**F**). *P<0.05 vs. *EphB2*$^{+/+}$ CTL. (**E**) Frozen kidney sections from *EphB2*$^{+/+}$ and *EphB2*$^{-/-}$ mice following IR injury were stained with EphB2 (red) and DAPI/DNA (blue). Magnification, ×200. There is no EphB2 detected in immunoblots or IF staining in kidneys from *EphB2* KO mice.

and *EphrinB2* ligands (see Supplementary Figure S1B). We then investigated potential changes in expression following IR injury and found that EphB2 mRNA and protein levels were significantly up-regulated in the WT IR-injured kidney compared with the uninjured control kidney (CTL) (Figure 1A–C). Consistent with this, immunoblots using a phospho-specific antibody for EphB1/EphB2 that provides a readout for tyrosine kinase catalytically active receptor (p-EphB1/2) detected a significant increase in the IR-injured WT mouse kidney (Figure 1B,D). IF analysis of tissue sections using anti-EphB2 antibodies confirmed an increase in receptor protein expression in the WT IR-injured kidney, particularly in the tubular epithelial cells and tubulointerstitial cells (Figure 1E). Importantly, no EphB2 signals were detected in immunoblots or IF in kidneys from *EphB2* KO mice (*EphB2*$^{-/-}$) demonstrating the specificity of the antibody reagents. Finally, significant increase in EphrinB2 protein expression was also detected in IR-injured kidney from WT mice, although interestingly this increase was not detected in injured kidneys from *EphB2* KO mice (Figure 1B,F).

To ascertain whether up-regulated expression of *EphB2* and *EphrinB* genes could also be observed in other animal models of kidney diseases, we subjected kidneys from type 2 diabetic *db*/*db* mice [27] and deoxycorticosterone acetate (DOCA) salt and angiotensin (Ang) II-infused hypertensive mice [22] to RT-PCR analysis. The data indicate that *EphB2*, *EphrinB1*, and *EphrinB2* transcripts were all significantly increased in the kidneys in both models (Supplementary Figure S2). We then carried out IF staining for EphB2 in kidney biopsies in CKD patients with a

Clinical Science (2021) **135** 2127–2142
https://doi.org/10.1042/CS20210644

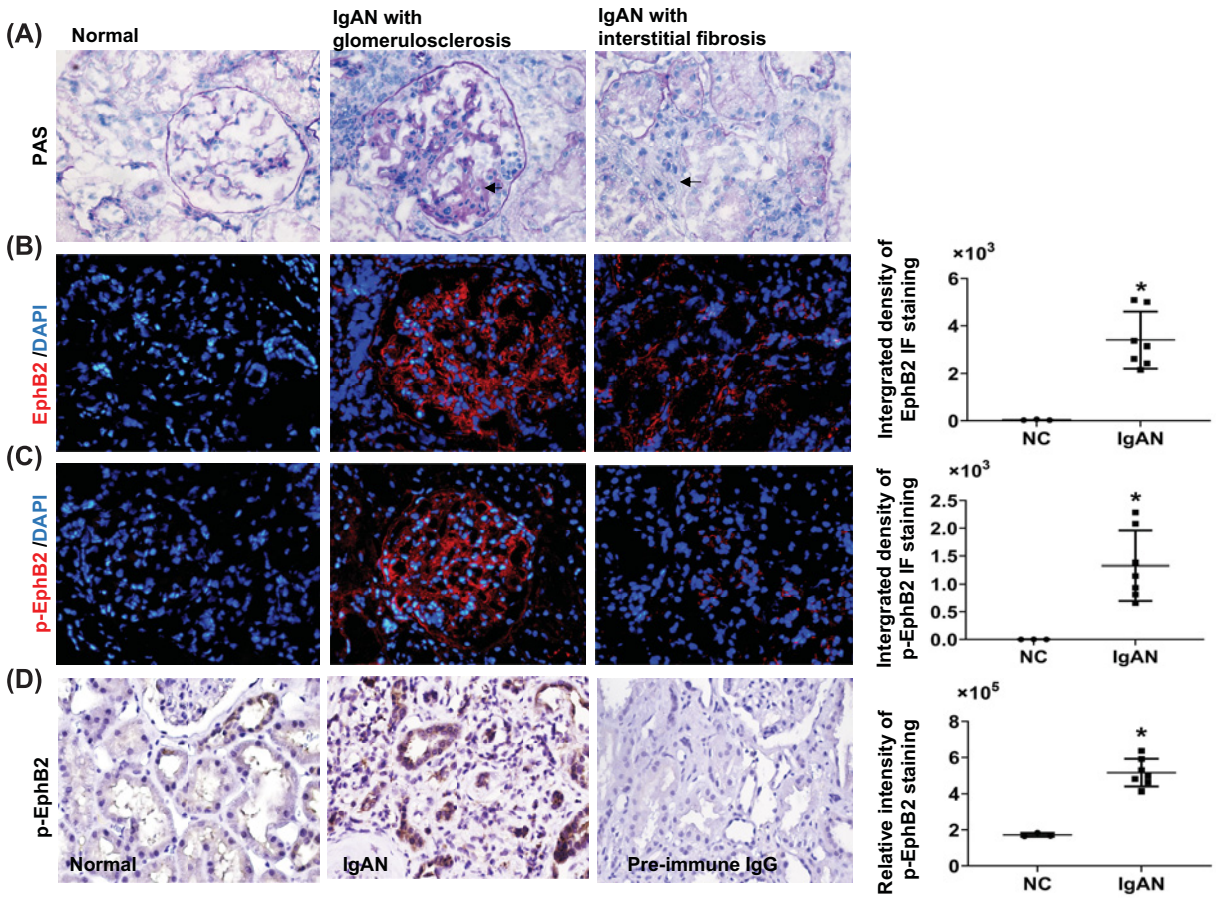

Figure 2. EphB2 expression increases in human kidney biopsy tissue with CKD compared with normal subjects

Kidney biopsy sections from normal part of kidney (NC, n=3) and the IgAN patients (Oxford pathological type T = 1 [38]) (n=7) from Nanjing Medical University were stained with PAS (**A**), EphB2 (red) (**B**), and phosphor-EphB2 (p-EphB2) (red) (**C**). Magnification, ×200. DAPI-stained DNA (blue) served as nuclei staining control for IF staining (IF staining was carried out as described for mouse tissue). Use of the human material was approved by the local ethical review board. Magnification ×200. Arrows indicated fibrosis in glomerulus and tubulointerstitial area. (**D**) Immunochemistry staining for p-EphB2 (stained in brown) (using the same anti-pEphB2 antibody as the primary antibody as used for IF staining and the peroxidase-conjugated anti-rabbit IgG (Jackson ImmunoResearch Laboratories Inc.) as the secondary antibody and positive staining was developed by using 3,3′-diaminobenzidine) was further carried out on 3-μm sections of paraffin-embedded these IgAN kidney biopsy tissues and was counterstained with Hematoxylin. As a negative control, the primary antibody was replaced by pre-immune IgG and no specific staining was noted. Magnification ×400. Relative integrated pixel density of the staining of the EphB2 or p-EphB2 specially in renal tubulointerstitial area, as quantified by ImageJ, was shown on the right of each staining photos. *P<0.05 vs. normal kidney (NC).

diagnosis of IgA nephropathy (IgAN) with glomerulosclerosis, tubular atrophy and interstitial fibrosis as determined by PAS staining (Figure 2A). Compared with normal subjects, a striking pattern of elevated EphB2 protein and forward signaling (staining with p-EphB1/2 antibodies) was detected not only in the diseased glomeruli but also in the disease-involved tubular area in the kidneys from these IgAN patients, (Figure 2B,C). Immunohistochemistry staining using the same anti-p-EphB2 antibody as used for IF staining further revealed that strong p-EphB2 staining was seen mainly in tubular cells and some in tubulointerstitial cells in these IgAN patients (Figure 2D). By contrast, only a few tubular cells were stained weakly for p-EphB2 in the normal kidney (Figure 2D). The semi-quantified integrated density levels for EphB2 or p-EphB2 staining in the renal tubulointerstitial area determined by ImageJ were shown on the right respectively. These data indicate that up-regulated expression of EphB2 and potential activation of forward signaling is a prominent feature of renal fibrosis.

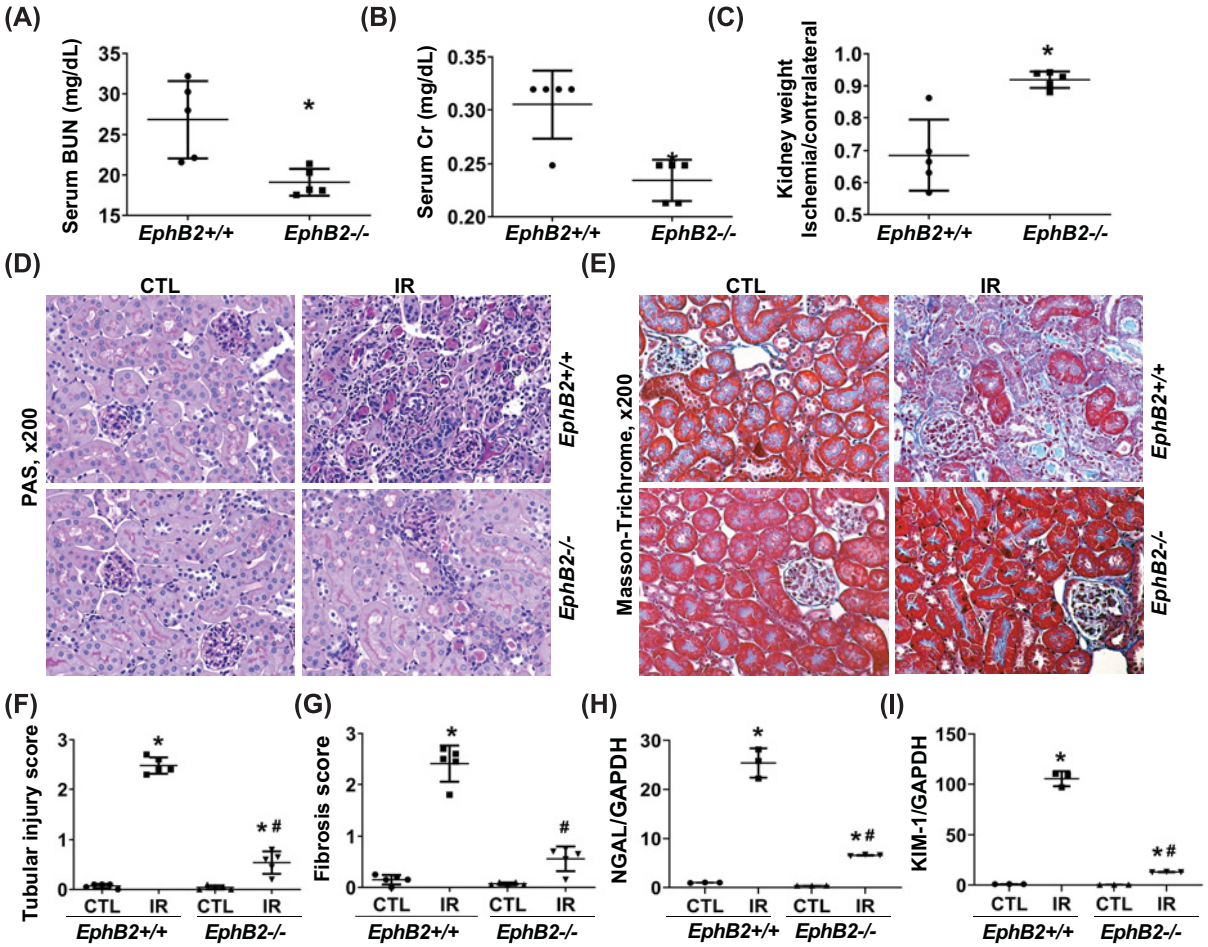

Figure 3. *EphB2*-KO mice exhibit ameliorated renal function and atrophy and reduced tubular injury and tubulointerstitial fibrosis following IR injury

(**A–C**) Serum BUN (A), Cr levels (B), and kidney weight (C) (n=5/group). *P<0.05 vs. *EphB2*$^{+/+}$ mice. (**D**,**E**) Representative microscopic images showing PAS staining (D) and Masson's Trichrome staining (E) of the kidney sections used to detect tubular injury, inflammation, and collagen deposition (stained blue). Magnification, ×200. (**F**,**G**). The graphs summarized the results of tubular injury (F) and collagen deposition (G) quantified by ImageJ. (**H**,**I**) mRNA expression of tubular injury markers, NGAL (H) and KIM-1 (I) in the kidney following IR injury. *P<0.05 vs. *EphB2*$^{+/+}$ contralateral kidney (CTL). #P<0.05 vs. *EphB2*$^{+/+}$ IR-injured kidney.

EphB2 KO protects kidney from IR-induced injury and fibrosis

In the IR model of kidney injury and fibrosis, a 35-min ischemia protocol in WT mice induced typical severe chronic unilateral kidney damage after 2 weeks, including impaired kidney function as evident by increased serum BUN and Cr levels (Figure 3A,B) (although the serum levels of BUN or Cr measured here only partially reflect the impaired function of the IR-injured kidney, both serum BUN and Cr levels in WT mice with unilateral renal IR injury were significantly increased compared with WT normal mice without any injury (BUN vs. Normal: 26.81 ± 4.25 vs. 17.3 ± 0.37 mg/dl; Cr: 0.301 ± 0.029 vs. 0.158 ± 0.064 mg/dl)) and kidney atrophy as evident by reduced kidney weight index (ratio of IR-injured kidney weight over control, uninjured kidney weight) (Figure 3C). Histologically, the IR-injured kidney in WT mice showed typical tubulointerstitial mononuclear cell infiltration and deposition of accumulated collagen as determined by PAS staining and Masson's Trichrome staining (Figure 3D–G). The IR-injured *EphB2*$^{-/-}$ mice showed a strong reduction in BUN and Cr levels compared with WT injured mice, and remarkably less kidney atrophy, tubular injury, and tubulointerstitial fibrosis. Renal transcripts for neutrophil gelatinase-associated lipocalin (*NGAL*) and kidney injury molecule-1 (*KIM-1*) mRNA were also assessed since both are validated as early predictive markers of renal tubular injury. The data indicated that while *NGAL* and *KIM-1* became very highly expressed in the IR-injured kidney from WT mice, their expression was markedly reduced by 77.2 and 88.5%, respectively, in the

Clinical Science (2021) **135** 2127–2142
https://doi.org/10.1042/CS20210644

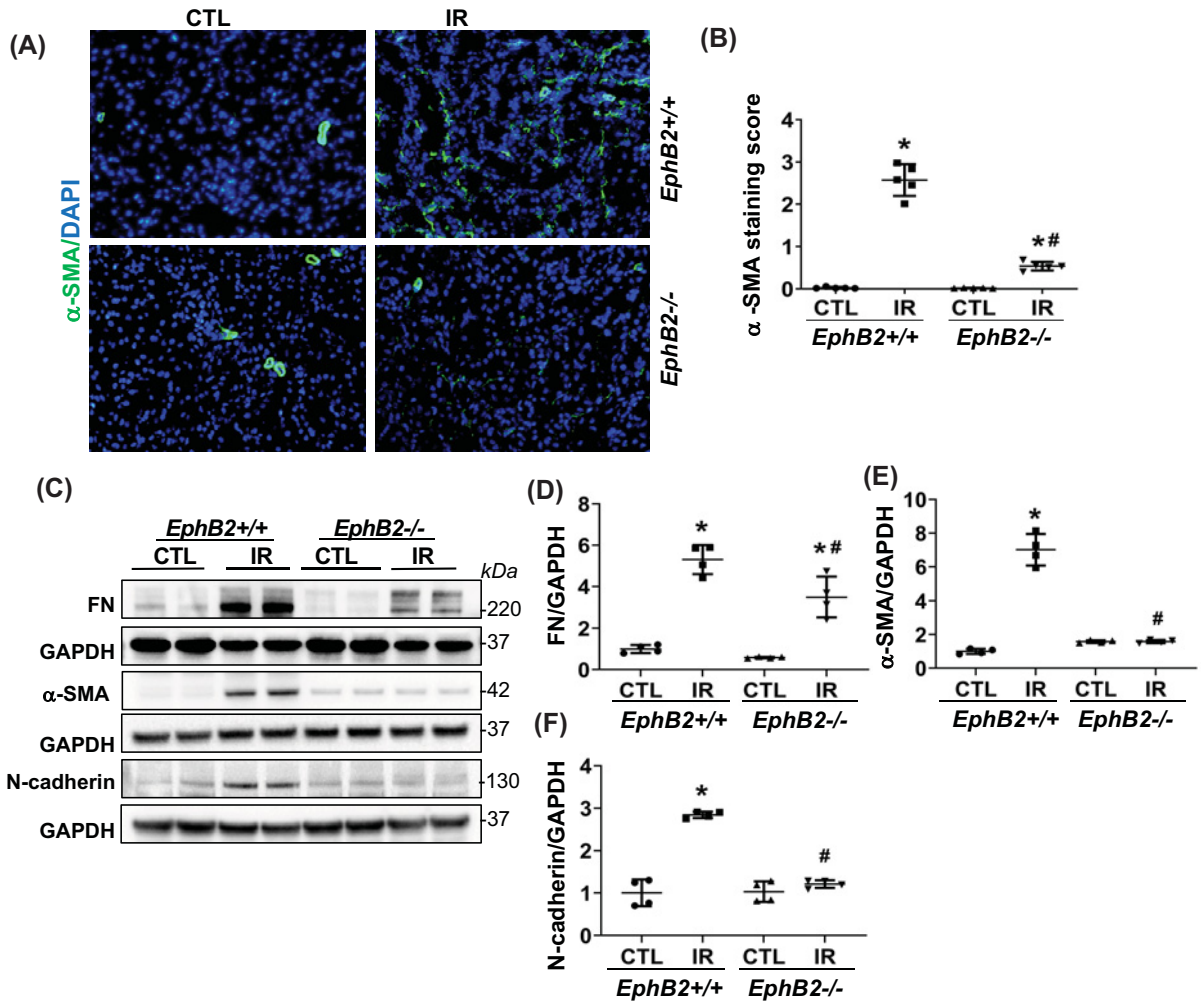

Figure 4. EphB2-KO mice have reduced tubular α-SMA staining and renal protein levels of fibrotic markers following IR injury

(**A**) Frozen kidney sections from *EphB2*$^{+/+}$ and *EphB2*$^{-/-}$ mice following IR injury were stained with α-SMA (red) and DAPI/DNA (blue) and analyzed using confocal microscopy. Magnification, ×200. (**B**) The graphs summarized the results of α-SMA deposition quantified by ImageJ. *P<0.05 vs. *EphB2*$^{+/+}$ contralateral kidney (CTL). (**C**) Western blots of FN, α-SMA, N-cadherin, and GAPDH from CTL and IR-injured kidneys of *EphB2*$^{+/+}$ and *EphB2*$^{-/-}$ mice. Molecular weight was labeled on the right. n=5 animals/group. (**D**–**F**) The graphs summarized the results of band density measurements for FN (D), α-SMA (E), and N-cadherin (F). *P<0.05 vs. *EphB2*$^{+/+}$ CTL. #P<0.05 vs. *EphB2*$^{+/+}$ IR-injured kidney.

injured kidneys from *EphB2*$^{-/-}$ mutant mice (Figure 3H-I). This indicates that tubular damage following IR injury was strongly reduced in mice that lacked expression of the EphB2 receptor.

α-SMA typically increases during differentiation of tubular cells into fibroblasts or activation of fibroblasts to myofibroblasts or vascular remodeling. Using IF analysis of kidney sections, we detected a marked increase in α-SMA staining in the tubular cells in IR-injured kidneys from WT mice, a response that was dramatically abrogated in *EphB2*$^{-/-}$ mice (Figure 4A,B). This observation was further supported by immunoblot analyses showing a striking reduction in the elevated protein levels of α-SMA as well as mesenchymal/fibrotic phenotype characterized by expression of N-cadherin, and FN in IR-injured kidneys from *EphB2*$^{-/-}$ mice compared with the WT controls (Figure 4C–F). Further analysis showed increased mRNA levels of the fibrotic markers including collagen type Iα1 (*Col-Iα1*), *Col-IIIα1*, *Col-IVα1*, and *FN* in the IR-injured kidney were also significantly reduced in the *EphB2*$^{-/-}$ mutants (Figure 5). These data indicate that *EphB2* KO protects kidney from IR-induced tubular EMT and fibrosis.

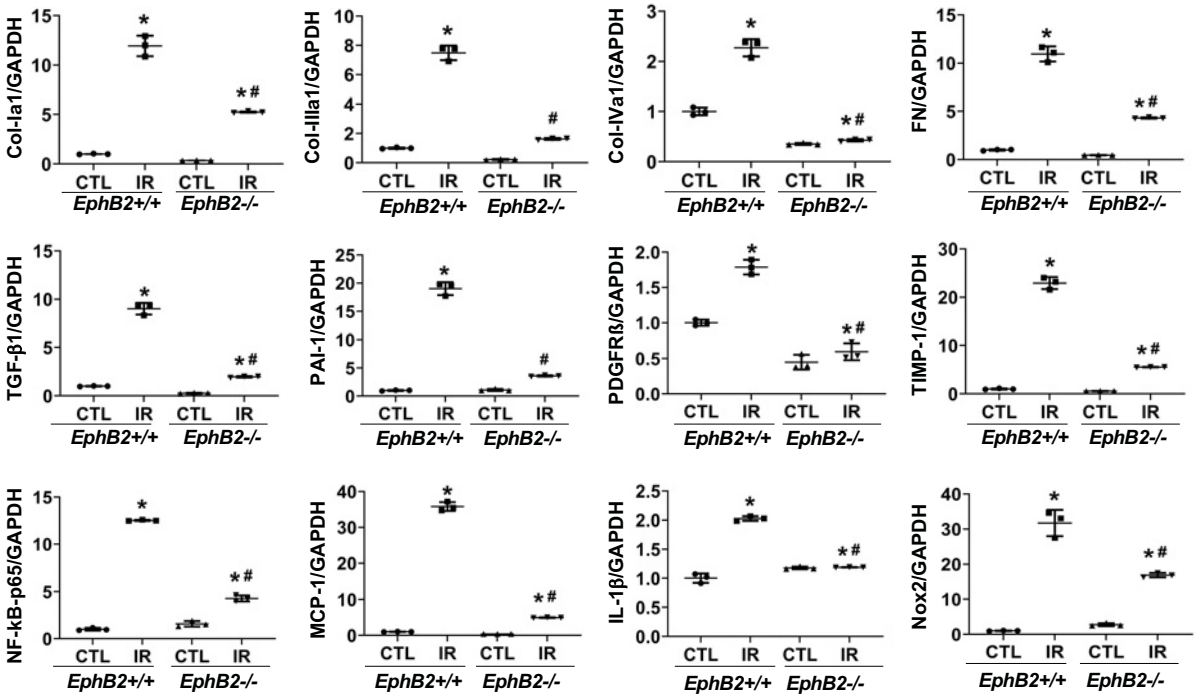

Figure 5. Quantitative RT-PCR for gene expression analysis of the profibrotic and inflammatory markers

Total RNA was prepared from contralateral (CTL) or IR-injured kidneys of *EphB2*$^{+/+}$ and *EphB2*$^{-/-}$ mice. Data are mean ± SD, n=5 animals per group. *P<0.05 vs. *EphB2*$^{+/+}$ CTL, #P<0.05 vs. *EphB2*$^{+/+}$ IR-injured kidney.

EphB2 KO mitigates a robust renal inflammatory, oxidative stress, and proliferative responses following IR injury

As key modulators of tissue fibrosis, TGFβ1, plasminogen-activator inhibitor type 1 (PAI-1), platelet-derived growth factor receptor-β (PDGFRβ), and tissue inhibitor of metalloproteinase (TIMP1) play an important role in renal fibrosis. As expected, renal mRNA levels of *TGFβ1*, *PAI-1*, *PDGFR-β*, and *TIMP1* were increased markedly in IR-injured kidneys of WT mice, compared with their internal CTL uninjured kidneys (Figure 5). However, mRNA expression of these profibrotic modulators was strongly blunted in IR-injured kidneys of *EphB2*$^{-/-}$ mice. These results are consistent with the reduction of renal fibrosis we observed in *EphB2*$^{-/-}$ mice following IR injury.

To further verify the effect of *EphB2* KO on related cellular downstream signaling pathways, we observed that renal RNA transcripts for *NF-κB-p65*, monocyte chemoattractant protein-1 (*MCP-1*), interleukin *(IL)-1β*, and *Nox2* were all increased in IR-injured kidneys of WT mice (Figure 5). Furthermore, renal protein production of NF-κB-p65, Nox2, and its cofactor, p47^{phox} was much greater in IR-injured kidneys of WT mice compared with CTL kidneys, indicating activation of NF-κB-mediated inflammatory pathway and Nox2 in the IR-injured kidney. However, levels of these mediators were ameliorated or reversed close to normal levels in KO mice lacking *EphB2* expression (Figure 6A–D). The phosphorylation and signaling of a serine/threonine kinase (Akt) and MAPK/ERK pathways were increased in IR-injured kidneys of WT mice, which were dramatically reduced, approaching normal levels, in *EphB2*$^{-/-}$ mice (Figure 6A,E,F). The F4/80 antibody, known to label macrophages, demonstrated a substantial increase in the absolute number of F4/80+ cells in tubulointerstitial area in IR-injured kidneys of WT mice, while F4/80+ cells were sparse in renal vessels in CTL kidneys, indicating an accumulation of macrophages and inflammation in damaged kidneys. However, the number of F4/80+ cells was largely reduced in *EphB2*$^{-/-}$ mice, approaching normal levels observed in uninjured kidneys (Figure 7A,B). Moreover, we tested for Ki-67, a nuclear protein that serves as a cellular marker of proliferation. Consistent with the activation of Akt and ERK1/2 in the IR-injured kidney of WT mice, IF staining detected a dramatic increase in Ki-67-positive cell number in tubulointerstitial area. In contrast, *EphB2*$^{-/-}$ mice exhibited a much lower number and less staining intensity of Ki-67 in IR-injured kidneys that more resembled the normal uninjured kidney (Figure 7C,D). These data indicate that deletion of *EphB2* inhibits NF-κB-mediated inflammation, NADPH oxidase-mediated oxidase generation and activation, and Akt- and ERK1/2-mediated cell

Clinical Science (2021) **135** 2127–2142
https://doi.org/10.1042/CS20210644

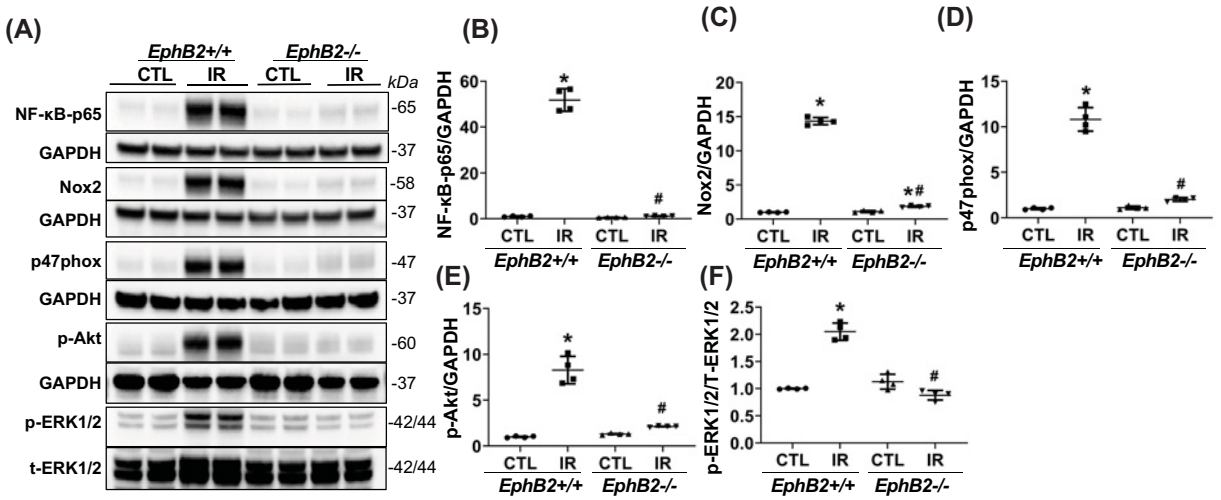

Figure 6. Renal protein levels of inflammatory, oxidative stress, and proliferative markers

(**A**) Western blots of NF-κBp65, Nox2, p47^{phox}, p-Akt, pERK1/2, t-ERK1/2, and GAPDH from contralateral (CTL) and IR-injured kidneys of *EphB2*$^{+/+}$ and *EphB2*$^{-/-}$ mice. Molecular weight was labeled on the right. n=5 animals/group. (**B–F**) The graphs summarized the results of band density measurements for NF-κB-p65 (B), Nox2 (C), p47^{phox} (D), p-Akt (E), pERK1/2/t-ERK1/2 (F), respectively. *P<0.05 vs. *EphB2*$^{+/+}$ CTL. #P<0.05 vs. *EphB2*$^{+/+}$ IR-injured kidney.

proliferation in the IR-injured kidney in mice. Thus, EphB2 might be required for the substantial renal inflammatory and proliferative responses that contribute to fibrosis.

Reduced apoptosis in the kidney of *EphB2*$^{-/-}$ mice following IR injury

Kidneys subjected to IR injury are also characterized by extensive renal tubular epithelial cell apoptosis. TUNEL staining displayed a significant elevation in apoptosis in IR-injured kidney sections of WT mice, compared with the CTL kidneys (Figure 8A,B), which was dramatically reduced in *EphB2*$^{-/-}$ mice. These results support a role of *EphB2* KO in suppressing apoptosis and repair mechanisms upon renal injury. Such additional effect of EphB2 may also explain the limited fibrosis that occurs in *EphB2*$^{-/-}$ mice following IR-induced chronic injury.

EphB2 signaling-related profibrotic pathway

Among the 760 genes tested by NanoString gene expression (shown in Figure 9A, a gene expression heatmap), there was evidence of differential gene expression (adjusted P<0.05) in the IR-injured kidney of WT mice relative to the WT CTL kidney (WT-IR vs. WT-CTL) for 506 genes (356 genes were up-regulated and 150 genes were down-regulated) with an estimated false discovery rate of 5%. The up-regulated 356 genes include all molecules that we have observed in their RNA expression or protein production using real time RT-PCR or Western blot assay described above and these genes encode for fibrotic markers such as Col-Iα1, Col-IIIα1, Col-IVα1, and FN; EMT markers such as α-SMA and vimentin; inflammatory factors and oxidative enzymes such as NF-κB, MCP-1, IL-1β, and Nox2; growth factors and proliferation markers such as TGFβ1, PAI-1, PGDFRβ1, TIMP-1, MEK kinase, Akt-1 and Ki-67, and caspase-3, -4, and -12 that regulate inflammation and apoptosis. However, all those increased markers that were significantly attenuated in the IR-injured kidney of *EphB2* KO mice compared with WT mice (KO-IR vs. WT-IR) determined by real time RT-PCR or Western blot assay described above are also confirmed by NanoString gene expression assay. The down-regulated genes include superoxide dismutase 1 (*SOD1*) [28], heme oxygenase 1 (*Hmox1*) [29], and thioredoxin 1, 2 (*Txn1, 2*) [30] that appear to be in the antioxidant family. Reduction in these genes is associated with the enhanced oxidative stress observed in the IR-injured WT kidney. However, such reduction in *SOD1* and *Txn1, 2* did not occur in the IR-injured *EphB2* KO kidney. Apparently, NanoString gene expression assay simultaneously uncovered multiple candidate genes that are involved in IR-induced renal injury and fibrosis. Notably, 230 of 356 up-regulated genes were reduced (total 64.6%↓, with adjusted P<0.05) and 129 of 150 down-regulated gene were reversed to varying degrees (total 86%↑, with adjusted P<0.05) in the IR-injured kidney of *EphB2*$^{-/-}$ mice compared with WT mice (KO-IR vs. WT-IR). All those ameliorated molecules are involved in 50 ameliorated annotated pathways (shown in Figure 9B, a heatmap of pathway scores). Among those, the common profibrotic pathways, shown

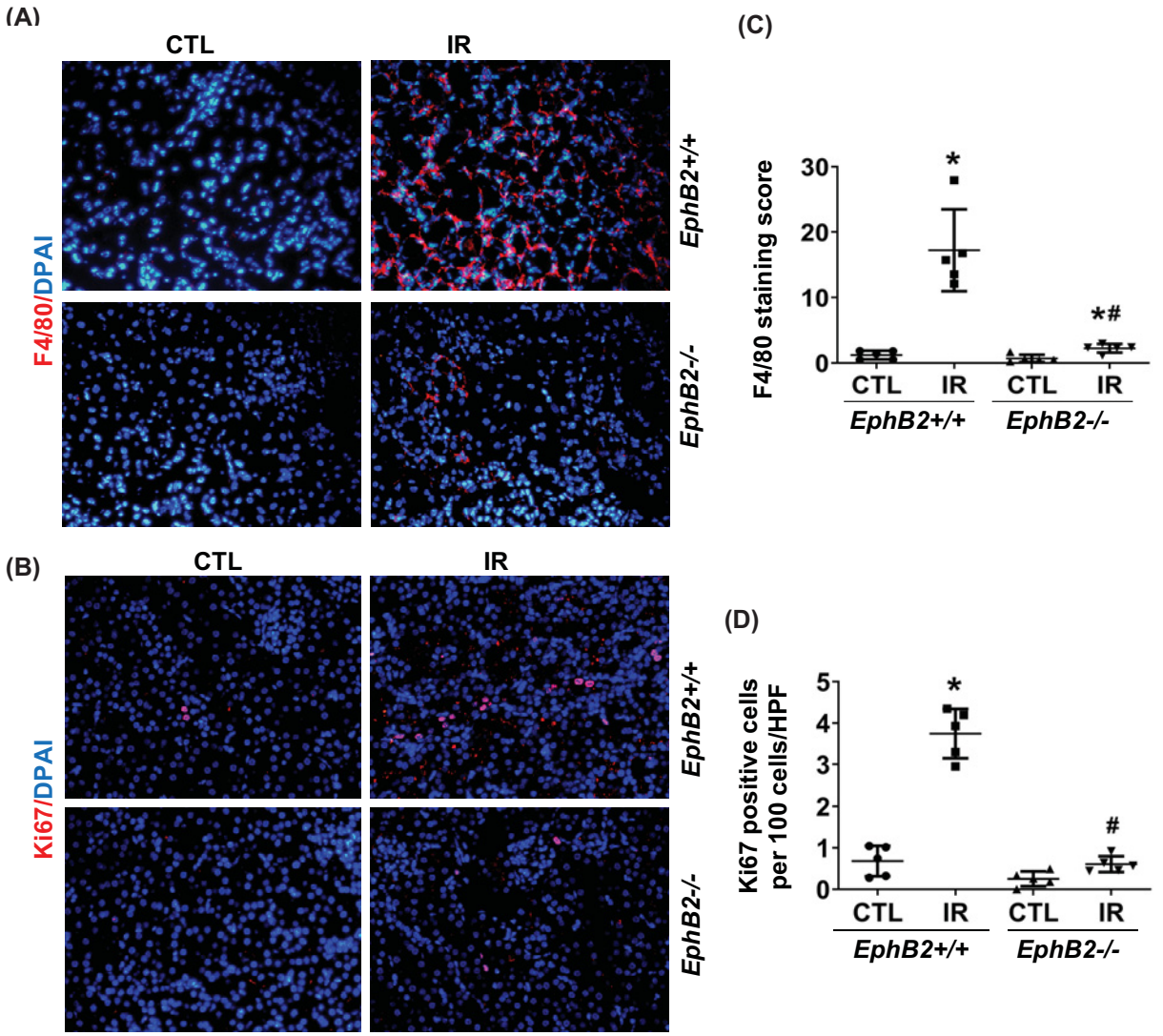

Figure 7. *EphB2* KO reduces macrophage infiltration and tubular cell proliferation in the kidney after IR injury

Kidney sections from *EphB2*$^{+/+}$ and *EphB2*$^{-/-}$ mice (n=5/each) following IR injury were stained with F4/80 (red) (**A**), Ki-67 (red) (**C**) and DAPI/DNA (blue) and analyzed using confocal microscopy. Magnification, ×200. The graphs summarized the results of F4/80^{+} (**B**) and Ki-67^{+} cells (**D**) quantified by ImageJ. $^{*}P<0.05$ vs. *EphB2*$^{+/+}$ contralateral kidney (CTL). $^{\#}P<0.05$ vs. *EphB2*$^{+/+}$ IR-injured kidney.

in Figure 9C, that well contribute to the development of renal fibrosis, such as the EMT and the inflammatory and proliferative pathways, are markedly activated or up-regulated in the IR-injured kidney, but significantly ameliorated in the IR-injured *EphB2* KO kidney. Surprisingly, this analysis also revealed that renal tubular cell energy metabolism such as *de novo* lipogenesis, gluconeogenesis, cholesterol metabolism, the peroxisome proliferator-activated receptor (PPAR) signaling, and particularly fatty acid metabolism in addition to the decreased mRNA expression of antioxidants (as listed as oxidative stress pathway in the heatmap, Figure 9B), largely destroyed in the IR-injured kidney, was dramatically persevered in the IR-injured *EphB2* KO kidney (as shown in Figure 9D). These results further suggest that the majority of molecules that are involved in renal injury and fibrosis are regulated by or related to the EphB2 signaling. Notably, the EphB2 signaling may be involved in or mediate renal tubular cell mitochondrial energy metabolism such as mitochondrial fatty acid oxidation and lipotoxicity in kidney diseases.

Clinical Science (2021) **135** 2127–2142
https://doi.org/10.1042/CS20210644

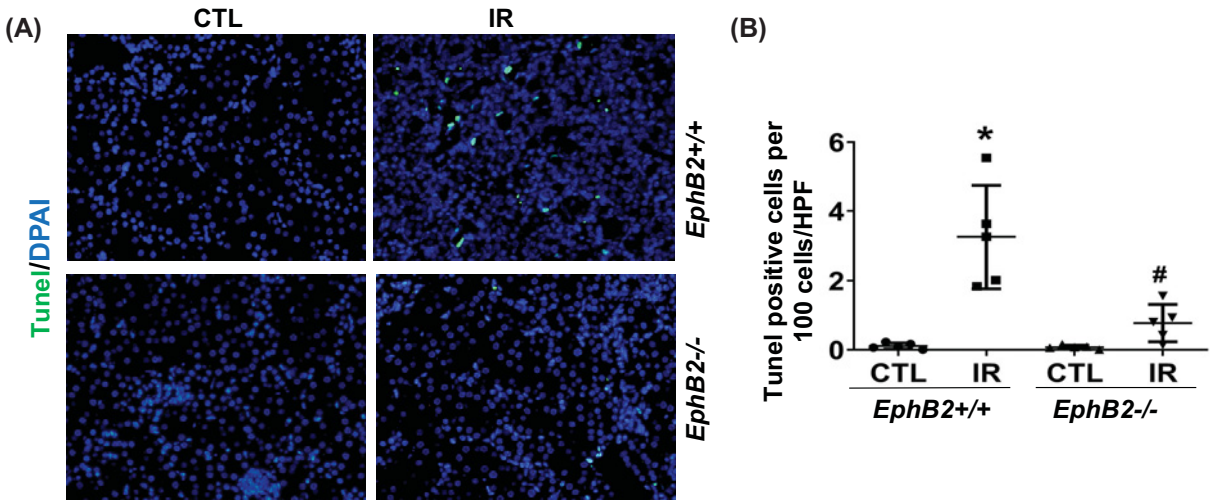

Figure 8. *EphB2* KO reduces tubular cell apoptosis in the kidney after ischemia-reperfusion (IR) injury

(**A**) Kidney sections from *EphB2*$^{+/+}$ and *EphB2*$^{-/-}$ mice (n=5/each) following IR injury were stained with TUNEL (green), and DAPI/DNA (blue) and analyzed using confocal microscopy. Magnification, ×200. (**B**) The graphs summarized the results of TUNEL^{+} cells quantified by ImageJ. *P<0.05 vs. *EphB2*$^{+/+}$ contralateral kidney (CTL). #P<0.05 vs. *EphB2*$^{+/+}$ IR-injured kidney.

Discussion

In the present study, we used the unilateral renal IR mouse model that is well established for studying the transition of renal actual kidney disease (AKI) to CKD [31,32]. Features of extensive inflammatory response, renal tubular epithelial cell apoptosis, and fibrosis were observed while EphB2 was up-regulated and activated at the site of IR injury in mouse kidney. Importantly, up-regulation and activation of EphB2 are consistently found in diabetes or hypertension-induced CKD mouse models and the human biopsy tissues showing glomerulosclerosis and interstitial fibrosis. These observations are consistent with ERCB data in the publicly available kidney transcriptome database, Nephroseq. mRNA expression levels of EphB2 in kidney procured from patients with FSGS were significantly higher than those in healthy living donors (www.nephroseq.org). Collectively, these data suggest that EphB2 up-regulation/activation may be a basic response to chronic injury-induced renal fibrosis, regardless of the initiating agent or disorder. Furthermore, EphB2 KO attenuates renal inflammation, and fibrosis induced by IR injury in mice and this amelioration is correlated with an overall reduction in profibrotic markers and inflammatory cytokines, oxidative stress, and tubular cell death. Our results indicate that EphB2 signaling is crucial in kidney injury and potentially contributes to the development of renal fibrosis. Our observation using the NanoString gene expression demonstrating that the majority of molecules involved in renal fibrosis are regulated by or related to EphB2 further supports its role as a critical driver of kidney damage following IR injury.

The mechanistic pathways involved in injury-induced EphB2 signaling and activation have not been thoroughly investigated. We postulate that injury-induced increased ligands such as EphrinB1 and EphrinB2 as we observed in the IR-injured mouse kidneys and diabetes or hypertension-induced CKD mouse models may activate the EphB2 receptor via enhanced interaction of Eph–Ephrin. In addition, a few studies have shown that activation of Notch signaling pathway regulates EphB2 through the glycogen synthase kinase 1 (GSK)3β- mediated suppression of Wnt-/β-catenin signaling in intestinal epithelial cells both *in vitro* and *in vivo* in various gene-manipulated mouse models [33,34]. Whether this pathway also regulates EphB2 in the kidney during injury is not investigated yet. Interestingly, GSK-3β has been recently implicated in the pathogenesis of kidney injury [35]. On the other hand, it is likely that up-regulation/activation of EphB2 upon kidney injury may aggravate kidney cell injury, death, and EMT and thereby causing renal fibrosis via multiple pathways, including potentiation of NF-κB-mediated inflammation response, activation of TGFβ1/Smad3-mediated EMT and other pathways, as indicated by the NanoString gene expression and verified by the signaling assessment in the present study.

As the kidney is a highly metabolic organ and uses high levels of adenosine triphosphate (ATP) to maintain electrolyte and acid–base homeostasis and reabsorb nutrients, energy depletion is a critical factor in the transition of renal AKI to CKD, even CKD to ESRD [36]. Although we did not measure renal ATP levels after IR injury in WT

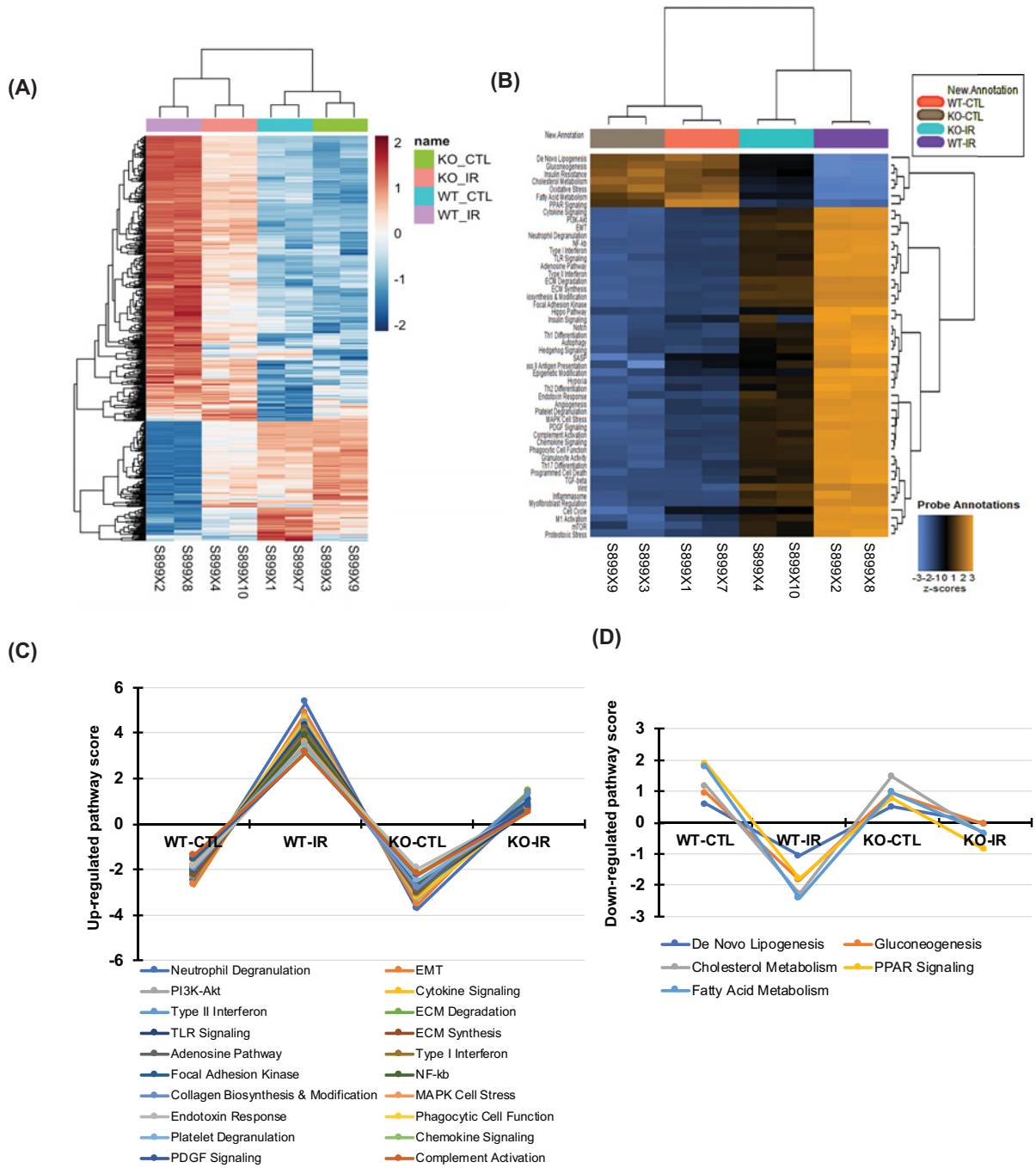

Figure 9. Heatmaps of differential gene expression and related pathway dysregulation scores for 760 genes in the kidney after IR injury analyzed by the NanoString mouse nCounter Fibrosis Panel

(**A**) Differential gene expression map in IR-injured kidney between *EphB2*$^{+/+}$ (WT) and *EphB2*$^{-/-}$ (KO) mice (n=5/each) compared with uninjured contralateral kidney (CTL), generated by using the *limma* software. (**B**) Dysregulation score map of 50 annotated fibrotic pathways in those kidneys generated by using nSlover™. (**C**) The top 20 up-regulated profibrotic pathways and (**D**) 5 down-regulated cellular energy metabolic pathways induced by IR injury were remarkably ameliorated when *EphB2* gene was deleted.

Clinical Science (2021) **135** 2127–2142
https://doi.org/10.1042/CS20210644

and *EphB2* KO mice, our brief observation using the NanoString gene expression in this model provides the first evidence that the EphB2 signaling may be involved in/or mediate renal tubular cell mitochondrial energy metabolism. Deletion of EphB2 signaling appears to largely prevent cellular energy damage thereby ameliorating cellular apoptosis and kidney fibrosis. These brief observations may suggest a new possible paradigm of EphB2 signaling in the pathogenesis of kidney fibrosis via induction of cellular energy metabolic dysfunction, especially tubular cell energy metabolic dysfunction, in addition to the injurious effects of EphB2 signaling on the inflammation and EMT. The metabolic pathway is also important and needs to be determined.

In the kidney, EphB2 is normally expressed in renal tubules [19]. Upon injuries, increased EphB2 was observed not only in proximal renal tubules but also in glomerular cells as we observed in kidney biopsy tissues from CKD patients. In IR-injured mouse kidneys, it is understandable that increased EphB2 is mainly observed in renal tubules since this injury mainly causes renal tubulointerstitial fibrosis. Of note, the process of kidney fibrosis involves multiple kidney cells, including renal tubular epithelial cells, interstitial fibroblasts, vascular ECs, and inflammation cells. In fact, besides being expressed on renal tubular cells and fibroblasts, EphB2 is also expressed in most cellular players of the immune system including monocytes/macrophages, dendritic cells, and B cells [37]. More research is underway to clearly delineate and understand the cell-specific function of Eph–Ephrin signaling axis during renal inflammation and fibrosis.

Different from other members of receptor tyrosine kinases, interaction of Eph–Ephrin activates bidirectional signaling cascades that are propagated into the receptor-expressing cell (forward signaling) and the ligand-expressing cell (reverse signaling) [3–5]. Recently, Ephrin-B2 reverse-signaling in blood vessels/capillaries was shown to be antifibrotic in the kidney after injury induced by UUO or IR since mice lacking the PDZ intracellular signaling domain of Ephrin-B2 exhibit increased kidney fibrosis [21]. However, this study cannot dissect whether the increased fibrosis is due to the PDZ-dead Ephrin-B2 protein acting as a stronger ligand to stimulate EphB receptors forward signaling. Similarly, the EphB2 deficiency data in the present study will not be able to dissect whether amelioration of renal fibrosis is related to abrogation of reverse signaling through Ephrin ligands. Despite the importance of EphB signaling in renal fibrosis found in our work, a further thorough understanding of how the EphB2/Ephrin signaling axis promotes renal fibrosis will be clearly warranted in the future.

In summary, the present study shows a direct involvement of EphB2 signaling in the pathogenesis of renal fibrosis using IR-induced renal fibrosis model in rodents. We also include our preliminary observations that EphB2 is markedly elevated in kidney biopsy tissue in patients with CKD, indicating its potential clinical importance. These findings suggest a novel and important link between up-regulation of EphB2 signaling and renal fibrosis and may open new avenues for targeting this receptor tyrosine kinase for the treatment of renal fibrosis.

Clinical perspectives

- Fibrosis is the major reason for destruction of the normal functioning of the kidney and results in CKD progression, with no preventive medicine available.
- We identified that the EphB2 receptor tyrosine kinase signaling was markedly activated at the site of injury in the kidneys from both CKD animal models and patients. Genetic loss of *EphB2* in KO mice strongly protected kidneys from IR-induced renal damage, dysfunction, and fibrosis, accompanied by reduction in multiple profibrotic pathways.
- These findings suggest a novel and important link between up-regulation of EphB2 signaling and renal fibrosis and may open new avenues for targeting this receptor tyrosine kinase for the treatment of renal fibrosis.

Data Availability

The models and reagents derived from this project will be made available to qualified investigators in the fields of chronic renal fibrosis upon their request and completion of a formal materials transfer agreement. Biologic material transfers will be made with no more restrictive terms than in the Uniform Biological MTA. We will willingly share our knowledge, protocol, and expertise when asked.

Competing Interests

The authors declare that there are no competing interests associated with the manuscript.

Funding

This work was supported by the American Diabetes Association [grant number 1-17-IBS-312 (to Yufeng Huang)]; and the NIH-NIDDK [grant numbers DK123727 (to Yufeng Huang), DK115991 (to Patrice N. Mimche)].

CRediT Author Contribution

Zhimin Huang: Data curation, Formal analysis, Validation, Investigation, Visualization, Methodology, Writing—review and editing. **Simeng Liu:** Data curation, Formal analysis, Validation, Investigation, Visualization, Methodology, Writing—review and editing. **Anna Tang:** Formal analysis, Methodology, Writing—review and editing. **Laith Al-Rabadi:** Writing—review and editing. **Mark Henkemeyer:** Resources, Writing—review and editing. **Patrice N. Mimche:** Conceptualization, Resources, Writing—review and editing. **Yufeng Huang:** Conceptualization, Resources, Data curation, Formal analysis, Supervision, Funding acquisition, Validation, Investigation, Visualization, Methodology, Writing—original draft, Project administration, Writing—review and editing.

Abbreviations

α-SMA, α-smooth muscle action; Ang II, angiotensin II; AKI, actual kidney disease; Akt, a serine/threonine protein kinase or protein kinase B; ATP, adenosine triphosphate; BUN, blood urea nitrogen; CKD, chronic kidney disease; Col-Ia1, collagen type 1 alpha 1; Cr, creatinine; DAPI, 4′,6-diamidino-2-phenylindole; DOCA, deoxycorticosterone acetate; EC, endothelial cell; ECM, extracellular matrix; EMT, epithelial-to-mesenchymal transition; Eph, erythropoietin producing hepatocellular; Ephrin, Eph receptor interacting; ERK, extracellular signal-regulated kinase; ESRD, end-stage renal disease; FN, fibronectin; FSGS, Focal segmental glomerulosclerosis; GAPDH, glyceraldehyde 3-phosphate dehyrogenase; GSK, glycogen synthase kinase 1; HMOX1, heme oxygenase 1; IF, immunofluorescent; IgAN, IgA nephropathy; IL, interleukin; IR, ischemia–reperfusion; KIM-1, kidney injury molecule-1; KO, knockout; MAPK, mitogen-activated protein kinase; MCP-1, monocyte chemoattractant protein-1; NF-kB-p65, nuclear factor k-B-p65 unite; NGAL, neutrophil gelatinase-associated lipocalin; Nox2, NADPH oxidase gp91^{phox} ; PAI-1, plasminogen-activator inhibitor type 1; PAS, Periodic Acid–Schiff; PDGF, platelet-derived growth factor; PDGFRβ, platelet-derived growth factor receptor-β; PDZ, post-synaptic density protein, disks large, zona occludens; PI3K/AKT, phosphatidylinositol 3-kinase/protein kinase B; PPAR, peroxisome proliferator-activated receptor; RT-PCR, reverse transcription-polymerase chain reaction; SOD1, superoxide dismutase 1; TGFβ, transforming growth factor-β; TIMP1, tissue inhibitor of metalloproteinase; TLR, toll-like receptor; TUNEL, TdT-mediated dUTP Nick-End Labeling; Txn1, thioredoxin 1; UUO, unilateral ureteral obstruction; WT, wildtype.

References

1 Mihai, S., Codrici, E., Popescu, I.D., Enciu, A.M., Albulescu, L., Necula, L.G. et al. (2018) Inflammation-related mechanisms in chronic kidney disease prediction, progression, and outcome. *J. Immunol. Res.* **2018**, 2180373, https://doi.org/10.1155/2018/2180373
2 Pasquale, E.B. (2008) Eph-ephrin bidirectional signaling in physiology and disease. *Cell* **133**, 38–52, https://doi.org/10.1016/j.cell.2008.03.011
3 Henkemeyer, M., Orioli, D., Henderson, J.T., Saxton, T.M., Roder, J., Pawson, T. et al. (1996) Nuk controls pathfinding of commissural axons in the mammalian central nervous system. *Cell* **86**, 35–46, https://doi.org/10.1016/S0092-8674(00)80075-6
4 Holland, S.J., Gale, N.W., Mbamalu, G., Yancopoulos, G.D., Henkemeyer, M. and Pawson, T. (1996) Bidirectional signalling through the EPH-family receptor Nuk and its transmembrane ligands. *Nature* **383**, 722–725, https://doi.org/10.1038/383722a0
5 Himanen, J.P., Rajashankar, K.R., Lackmann, M., Cowan, C.A., Henkemeyer, M. and Nikolov, D.B. (2001) Crystal structure of an Eph receptor-ephrin complex. *Nature* **414**, 933–938, https://doi.org/10.1038/414933a
6 Hafner, C., Schmitz, G., Meyer, S., Bataille, F., Hau, P., Langmann, T. et al. (2004) Differential gene expression of Eph receptors and ephrins in benign human tissues and cancers. *Clin. Chem.* **50**, 490–499, https://doi.org/10.1373/clinchem.2003.026849
7 Park, I. and Lee, H.S. (2015) EphB/ephrinB signaling in cell adhesion and migration. *Mol. Cells* **38**, 14–19, https://doi.org/10.14348/molcells.2015.2116
8 Salvucci, O. and Tosato, G. (2012) Essential roles of EphB receptors and EphrinB ligands in endothelial cell function and angiogenesis. *Adv. Cancer Res.* **114**, 21–57, https://doi.org/10.1016/B978-0-12-386503-8.00002-8
9 Yang, J.S., Wei, H.X., Chen, P.P. and Wu, G. (2018) Roles of Eph/ephrin bidirectional signaling in central nervous system injury and recovery. *Exp. Ther. Med.* **15**, 2219–2227, https://doi.org/10.3892/etm.2018.5702
10 Wu, B., Rockel, J.S., Lagares, D. and Kapoor, M. (2019) Ephrins and Eph receptor signaling in tissue repair and fibrosis. *Curr. Rheumatol. Rep.* **21**, 23, https://doi.org/10.1007/s11926-019-0825-x
11 Finney, A.C., Funk, S.D., Green, J.M., Yurdagul, Jr, A., Rana, M.A., Pistorius, R. et al. (2017) EphA2 expression regulates inflammation and fibroproliferative remodeling in atherosclerosis. *Circulation* **136**, 566–582, https://doi.org/10.1161/CIRCULATIONAHA.116.026644
12 Su, S.A., Yang, D., Wu, Y., Xie, Y., Zhu, W., Cai, Z. et al. (2017) EphrinB2 regulates cardiac fibrosis through modulating the interaction of Stat3 and TGF-beta/Smad3 signaling. *Circ. Res.* **121**, 617–627, https://doi.org/10.1161/CIRCRESAHA.117.311045

13 Nunan, R., Campbell, J., Mori, R., Pitulescu, M.E., Jiang, W.G., Harding, K.G. et al. (2015) Ephrin-Bs drive junctional downregulation and actin stress fiber disassembly to enable wound re-epithelialization. *Cell Rep.* **13**, 1380–1395, https://doi.org/10.1016/j.celrep.2015.09.085
14 Selman, M., Pardo, A. and Kaminski, N. (2008) Idiopathic pulmonary fibrosis: aberrant recapitulation of developmental programs? *PLoS Med.* **5**, e62, https://doi.org/10.1371/journal.pmed.0050062
15 Mimche, P.N., Brady, L.M., Bray, C.F., Lee, C.M., Thapa, M., King, T.P. et al. (2015) The receptor tyrosine kinase EphB2 promotes hepatic fibrosis in mice. *Hepatology* **62**, 900–914, https://doi.org/10.1002/hep.27792
16 Mimche, P.N., Lee, C.M., Mimche, S.M., Thapa, M., Grakoui, A., Henkemeyer, M. et al. (2018) EphB2 receptor tyrosine kinase promotes hepatic fibrogenesis in mice via activation of hepatic stellate cells. *Sci. Rep.* **8**, 2532, https://doi.org/10.1038/s41598-018-20926-9
17 Hashimoto, T., Karasawa, T., Saito, A., Miyauchi, N., Han, G.D., Hayasaka, K. et al. (2007) Ephrin-B1 localizes at the slit diaphragm of the glomerular podocyte. *Kidney Int.* **72**, 954–964, https://doi.org/10.1038/sj.ki.5002454
18 Takahashi, T., Takahashi, K., Gerety, S., Wang, H., Anderson, D.J. and Daniel, T.O. (2001) Temporally compartmentalized expression of ephrin-B2 during renal glomerular development. *J. Am. Soc. Nephrol.* **12**, 2673–2682, https://doi.org/10.1681/ASN.V12122673
19 Ogawa, K., Wada, H., Okada, N., Harada, I., Nakajima, T., Pasquale, E.B. et al. (2006) EphB2 and ephrin-B1 expressed in the adult kidney regulate the cytoarchitecture of medullary tubule cells through Rho family GTPases. *J. Cell Sci.* **119**, 559–5570, https://doi.org/10.1242/jcs.02777
20 Freywald, A., Sharfe, N. and Roifman, C.M. (2002) The kinase-null EphB6 receptor undergoes transphosphorylation in a complex with EphB1. *J. Biol. Chem.* **277**, 3823–3828, https://doi.org/10.1074/jbc.M108011200
21 Kida, Y., Ieronimakis, N., Schrimpf, C., Reyes, M. and Duffield, J.S. (2013) EphrinB2 reverse signaling protects against capillary rarefaction and fibrosis after kidney injury. *J. Am. Soc. Nephrol.* **24**, 559–572, https://doi.org/10.1681/ASN.2012080871
22 Tian, M., Tang, L., Wu, Y., Beddhu, S. and Huang, Y. (2018) Adiponectin attenuates kidney injury and fibrosis in deoxycorticosterone acetate-salt and angiotensin II-induced CKD mice. *Am. J. Physiol. Renal Physiol.* **315**, F558–F571, https://doi.org/10.1152/ajprenal.00137.2018
23 Zhou, G., Wu, J., Gu, C., Wang, B., Abel, E.D., Cheung, A.K. et al. (2018) Prorenin independently causes hypertension and renal and cardiac fibrosis in cyp1a1-prorenin transgenic rats. *Clin. Sci. (Lond.)* **132**, 1345–1363, https://doi.org/10.1042/CS20171659
24 Huang, Y., Border, W.A., Yu, L., Zhang, J., Lawrence, D.A. and Noble, N.A. (2008) A PAI-1 mutant, PAI-1R, slows progression of diabetic nephropathy. *J. Am. Soc. Nephrol.* **19**, 329–338, https://doi.org/10.1681/ASN.2007040510
25 Kulkarni, M.M. (2011) Digital multiplexed gene expression analysis using the NanoString nCounter system. *Curr. Protoc. Mol. Biol.* Chapter 25:Unit25B 10s94, 1–17, https://doi.org/10.1002/0471142727.mb25b10s94
26 Andres, A.C., Munarini, N., Djonov, V., Bruneau, S., Zuercher, G., Loercher, S. et al. (2003) EphB4 receptor tyrosine kinase transgenic mice develop glomerulopathies reminiscent of aglomerular vascular shunts. *Mech. Dev.* **120**, 511–516, https://doi.org/10.1016/S0925-4773(02)00461-6
27 Tang, L., Wu, Y., Tian, M., Sjostrom, C.D., Johansson, U., Peng, X.R. et al. (2017) Dapagliflozin slows the progression of the renal and liver fibrosis associated with type 2 diabetes. *Am. J. Physiol. Endocrinol. Metab.* **313**, E563–E576, https://doi.org/10.1152/ajpendo.00086.2017
28 Fukai, T. and Ushio-Fukai, M. (2011) Superoxide dismutases: role in redox signaling, vascular function, and diseases. *Antioxid. Redox Signal.* **15**, 1583–1606, https://doi.org/10.1089/ars.2011.3999
29 Poss, K.D. and Tonegawa, S. (1997) Reduced stress defense in heme oxygenase 1-deficient cells. *Proc. Natl. Acad. Sci. U.S.A.* **94**, 10925–10930, https://doi.org/10.1073/pnas.94.20.10925
30 Holmgren, A. (2000) Antioxidant function of thioredoxin and glutaredoxin systems. *Antioxid. Redox Signal.* **2**, 811–820, https://doi.org/10.1089/ars.2000.2.4-811
31 Zager, R.A., Johnson, A.C. and Becker, K. (2011) Acute unilateral ischemic renal injury induces progressive renal inflammation, lipid accumulation, histone modification, and "end-stage" kidney disease. *Am. J. Physiol. Renal Physiol.* **301**, F1334–F1345, https://doi.org/10.1152/ajprenal.00431.2011
32 Le Clef, N., Verhulst, A., D'Haese, P.C. and Vervaet, B.A. (2016) Unilateral renal ischemia-reperfusion as a robust model for acute to chronic kidney injury in mice. *PLoS ONE* **11**, e0152153, https://doi.org/10.1371/journal.pone.0152153
33 Koo, B.K., Lim, H.S., Chang, H.J., Yoon, M.J., Choi, Y., Kong, M.P. et al. (2009) Notch signaling promotes the generation of EphrinB1-positive intestinal epithelial cells. *Gastroenterology* **137**, 145–155, https://doi.org/10.1053/j.gastro.2009.03.046
34 Batlle, E., Henderson, J.T., Beghtel, H., van den Born, M.M., Sancho, E., Huls, G. et al. (2002) Beta-catenin and TCF mediate cell positioning in the intestinal epithelium by controlling the expression of EphB/ephrinB. *Cell* **111**, 251–263, https://doi.org/10.1016/S0092-8674(02)01015-2
35 Chen, B., Wang, P., Liang, X., Jiang, C., Ge, Y., Dworkin, L.D. et al. (2021) Permissive effect of GSK3beta on profibrogenic plasticity of renal tubular cells in progressive chronic kidney disease. *Cell Death Dis.* **12**, 432, https://doi.org/10.1038/s41419-021-03709-5
36 Jang, H.S., Noh, M.R., Kim, J. and Padanilam, B.J. (2020) Defective mitochondrial fatty acid oxidation and lipotoxicity in kidney diseases. *Front. Med. (Lausanne)* **7**, 65, https://doi.org/10.3389/fmed.2020.00065
37 Darling, T.K. and Lamb, T.J. (2019) Emerging roles for Eph receptors and Ephrin ligands in immunity. *Front. Immunol.* **10**, 1473, https://doi.org/10.3389/fimmu.2019.01473
38 Roberts, I.S., Cook, H.T., Troyanov, S., Alpers, C.E., Working Group of the International Ig ANN, The Renal Pathology Society et al. (2009) The Oxford classification of IgA nephropathy: pathology definitions, correlations, and reproducibility. *Kidney Int.* **76**, 546–556, https://doi.org/10.1038/ki.2009.168